



**CATECHIN/AG/TITANIA (CAT NPS) NANOPARTICLES AS NOVEL  
ANTIFOULING COMPOUND AGAINST BIOFILM FORMING  
BACTERIA OF VISAKHAPATNAM COAST, ANDHRA PRADESH, INDIA**

**G. Sravan Kumar<sup>1\*</sup> Ilahi Shaik<sup>2</sup> D. Sunil Kumar<sup>3</sup>**

<sup>1</sup>Department of Biotechnology, Gayatri Vidya Parishad College for Degree and P.G. Courses (A), Visakhapatnam, Andhra Pradesh-530045

<sup>2</sup>Department of Biochemistry, Gayatri Vidya Parishad College for Degree and P.G. Courses (A), Visakhapatnam, Andhra Pradesh-530045

<sup>3</sup>Department of Marine Living Resources, Andhra University, Visakhapatnam- 530 003

\*Corresponding Author Email: sravang2010@gmail.com

---

**Article History: Received: 12-03-2023      Revised: 14-05-2023      Published: 27-05-2023**

---

### **Abstract**

In the realm of nanotechnology, there is a need for the creation of novel experimental procedures for the production of nanoparticles. The sol-gel process was used to synthesize Catechin-Ag-Titania nanoparticles. Catechin-Ag-Titania NPs is proposed as a novel cost-effective and ecofriendly antifouling compound. Well-dispersed Catechin-Ag-Titania NPs designated as CAT NP has been achieved through catechin mediated reduction of silver and TiO<sub>2</sub> ions at ambient temperature. The CAT NP showed effective antifouling activity against the screened biofilm forming bacteria. SEM, XRD, FTIR and TEM showed the properties of CAT NP and antifouling properties of CAT NP will provide new opportunities to develop cost-effective and ecofriendly antifouling composition that is 10 times effective compared with control.

**Keywords:** CAT NP, Catechin, Ag, Titania, TEM.

---

**DOI: 10.48047/ecb/2023.12.Si5.365**

### **Introduction**

Nanotechnology is an evolving technology that has contributed towards the development of great diversity of materials. It entails the production and utilization of extremely small particles about 1–100 nm in size, where the synthesis of these particles is controlled or modified at the molecular level (Badawy *et al.*, 2010). The extreme size and the bottom-up approach to synthesize new materials (Rolison, 2003) are the two special factors of nanoparticles, which are making them the building blocks of next generation. During the recent years, approximately 200 products which contain engineered nano material in them were introduced into the market (Breggin *et al.*, 2007). Due to their desirable material characteristics and significant potential in a variety of applications, the synthesis of different nanostructures and titanium nanoparticles has attracted attention in recent years (Mills *et al.*, 1993). Among the existing photo catalytic materials TiO<sub>2</sub> NPs are considered to be the best. The reasons attributing to this photo catalytic nature is strong oxidizing power, prolonged thermodynamic stability and relative non-toxicity (Krishna *et al.*, 2006).

For the synthesis of nanoparticles, biological approaches are regarded as secure, economical, long-lasting, and environmentally benign processes (Schmid, 2011). Many bacteria, fungi, and

plants have been used to successfully create silver nanoparticles, including Kalimuthu *et al.*, in 2008, Chaudhari *et al.*, in 2012, Saifuddin in 2009, Kathiresan *et al.*, in 2009, and Raut *et al.*, in 2010 and Masurkar *et al.*, in 2011. By adding coatings or capping agents and functionalizing their surface, NMs can also be manipulated and distinguished from one another. Consequently, two particles of the same substance that are varied in size and shape may have various physical and chemical characteristics and applications (Tiede *et al.*, 2009; Ju-Nam and Lead, 2008). Numerous commercial products contain titanium dioxide nanoparticles (TiO<sub>2</sub>-NPs), which are currently produced in large quantities around the world. The formation of nanoparticles in different sizes and varied chemical compositions and regulated mono-dispersities is a fundamental topic in nanotechnology study. The need to create ecologically friendly nanoparticle manufacturing methods is currently increasing. The current study focuses on synthesis of novel nanocompound of catechin from plant extract, silver doped with Titania as antifouling agent.

## **Materials and methods**

### **Preparation of Catechin-Silver-TiO<sub>2</sub>Nanoparticles**

In brief, 50 ml of pure ethanol was mixed vigorously with 20 mM tetra butyl orthotitanate to create a solution. After stirring for 20 minutes at room temperature, 3 mM concentrated HNO<sub>3</sub> was added. The reaction mixture was then supplemented with 1Mm of Catechin powder and 1Mm of AgNO<sub>3</sub> (the molar ratio of Catechin to Silver was 1:1) while being continuously stirred for 60 minutes until Silver Nitrate and Catechin Powder had dissolved. The aforementioned solution was then injected with 2mL of deionized water. The obtained mixture of the solution was then kept for 2hours at room temperature while being constantly stirred to create a gel, which was then left to set for 12 hours. The Catechin/Ag/TiO<sub>2</sub> sample is first dried at 80°C over the course of a night before being annealed at 400°C for three hours in order to produce a greyish material.

### **Determination of Minimum Inhibitory Concentrations (MICs) by agar dilution (slight modification)**

Mueller-Hinton agar was prepared as per the conventional method. The sterilized agar was allowed to cool in water bath to 50°C. Dilutions of antimicrobial agents were prepared in 25–30 ml vials. To each container, 19 ml of molten agar was poured, carefully mixed and then these contents were poured into sterile Petri plates with pre-printed labels on a flat surface. The plates were allowed to dry so that there were no moisture traces on the agar surface and then cooled to room temperature. Care should be taken that the plates are not over dried. The inoculum density was set to a uniform 10<sup>4</sup> colony-forming units (CFU) per agar spot. Nearly four or five pure culture colonies were used to prevent choosing an unusual variation. Either overnight colonies emulsification from an agar medium or by diluting a broth culture inoculum can be prepared. After inoculation, the plates were incubated for 18 hours at 35–37°C in air. Minimum Inhibitory Concentration is nothing but the lowest concentration of an agent that fully suppresses observable growth that could be determined by a naked eye. It is to be noted that neither a single colony nor a thin haze inside the region of an infected spot should ever be taken into account for determining it.

## **SEM analysis**

The treatment of the iron panels followed the process outlined by Novitsky and MacSween (1989). A mixture of 2.5 percent glutaraldehyde, 85 percent filter-sterilized seawater, and 15 percent distilled water was used to fix iron panels. After fixing, salt crystals were removed from the iron panels by periodically washing them in double-distilled, sterile water. The grains were dehydrated in two stages using HMDS (hydroxyl hexamethyl di silazane) and a graded ethanol series (90% for 5 min). The iron panels were sputter-coated with gold after drying, and double-sided conductive tape was used to link them to SEM stubs.

### **Transmission electron microscopy**

The electron source for the TEM is a tungsten filament cathode fitted with an electron pistol that emits a high voltage electron stream. Electrostatic and electromagnetic lenses focus the electron beam's acceleration (from 40 to 100 kV) so that it is directed at the object under observation. In proportion to the density of the sample, some electrons in the electron beam will scatter when they hit the specimen. Unscattered electrons that pass through the specimen will strike a fluorescent viewing screen that is covered in either phosphor or zinc sulfide. The varying shades of blackness in the resulting image are related to the sample density and dispersed electrons.

### **X-Ray diffraction analysis**

The technique known as X-ray diffraction analysis (XRD) is employed to examine size and structure of crystals. At the Advanced Analytical Laboratory at Andhra University, XRD analysis using a Siemens D5000 diffractometer provided further details about particle size and crystal structure.

### **Results and Discussion**

Recently, *Nyctanthes arbor-tristis* extract and other natural products have been used to create green TiO<sub>2</sub> nanoparticles (Jha *et al.*, 2009). Ag NPs can be produced on TiO<sub>2</sub> surfaces via photochemical, sol-gel techniques, aqueous reduction and liquid phase deposition (Cozzoli *et al.*, 2004; Guin *et al.*, 2007). Natural products such as *Eclipta prostrate* aqueous leaf extract, *Nyctanthes arbor-tristis* extract, *Catharanthus roseus* aqueous leaf extract, and *Aspergillus flavus* aqueous extract have all been used in the synthesis of TiO<sub>2</sub> NPs (Sundrarajan and Gowri, 2011, Velayutham *et al.*, 2012, Kirthi *et al.*, 2011). According to Adams, *et al.*, (2006) and Long, *et al.*, (2006), TiO<sub>2</sub> is one of the best opacifiers and is used as a pigment in paints, inks, paper, sunscreens, cosmetics, and plastics. Additionally, several researchers have developed silver supported Titania materials as a photo catalytic bactericide using these fundamentals and the antibacterial properties of silver (Castro *et al.*, 2002; Chao *et al.*, 2003 and Akhavan, 2009). Using silver nitrate precursor and catechin, we created silver nanoparticles supported on Titania by sol-gel in the current study.

Data were compared using the XRD patterns for synthetic TiO<sub>2</sub> NPs and the control sample of pure TiO<sub>2</sub> (Figure 1). About 25.35, 38.08, 48.08, 54.19, 54.95, 62.63, 68.21, 70.39, 74.94, and 82.73 are the well-defined diffraction peaks with 2 $\theta$ , which are ascribed to the (101), (004), (200), (105), (211), (204), (116), (220), (215), and (224) crystal planes, respectively. This XRD characteristic pattern is compatible with the typical JCPDS values of anatase TiO<sub>2</sub> (JCPDS Card No. 21-1272) (Maduda *et al.*, 2009 and Ge *et al.*, 2006), tetragonal structure, and did not occur in rutile and brookite form. Using Scherrer's formula, the average crystallite size of nanoparticle

samples was determined from FWHM of the anatase (101) reflection plane (Figure 1) (Dhage *et al.*, 2004). The Ag NPs produced by our environmentally friendly approach were nanocrystalline in nature, as shown by the occurrence of structural peaks in XRD patterns and average crystalline size of roughly 22 nm. Debye-Scherrer equation can be used to determine the average particle size of silver nanoparticles produced by the current green approach (Ahmad *et al.*, 2010; Vidhu *et al.*, 2011).

$$d = K\lambda/\beta\cos\theta,$$

Here in the above equation,  $d$  represents crystallite size,  $K$  represents constant ( $=0.9$ , assuming the particles to be spherical),  $\lambda$  is wavelength of X-ray diffraction.  $\beta$  is the FWHM and the angle of diffraction is represented by  $\theta$ . The samples that were synthesized possessed small crystallite sizes, with an average size of 19 nm, according to the predicted crystallite size, it was discovered. From this, it is clear that the catechin and silver additions somewhat reduced the size of the  $\text{TiO}_2$  crystallites. Comparing (101) reflection plane of pure  $\text{TiO}_2$  with Catechin, Silver, and  $\text{TiO}_2$ , it can be seen that the inclusion of Catechin and silver into  $\text{TiO}_2$  has a broadening effect, which may account for the decrease in  $\text{TiO}_2$  particle size. The predicted crystallite size decreased as the intensity was decreased and the width of the (101) reflection plane was increased. Additionally, the Catechin/Silver/ $\text{TiO}_2$  samples' (101) reflection plane changed to a greater diffraction angle in comparison to pure  $\text{TiO}_2$  (Figure1). The measured values can be used to calculate the lattice parameter ( $a$ ) for the spacing of the (111) plane, respectively. The results of the lattice parameter and the inter planer spacing's measured in the XRD analysis, the lattice constriction was found as represented in Table 1.

In an attempt to determine the functional groups of catechin/Ag/ $\text{TiO}_2$  nanoparticles and pure  $\text{TiO}_2$  NPs, the FTIR spectra of the nanoparticles were taken. FTIR spectra of catechin and silver co-doped  $\text{TiO}_2$  nanoparticles and un-doped  $\text{TiO}_2$  are displayed in (Figure 2 and 3) respectively. Undoped  $\text{TiO}_2$ 's spectra contained significant absorbance bands at 3387, 2925, 2853, 1627, 1383, 662, 626, 584, and 552  $\text{cm}^{-1}$ . The O-H group's stretching vibrations in undoped  $\text{TiO}_2$  could be responsible for the broad band that was seen at 3387, 2925, and 2853  $\text{cm}^{-1}$ . The bands at 2853 $\text{cm}^{-1}$  depict the asymmetric stretching, scissoring, twisting, and rocking vibrations of methylene groups, respectively. The distinctly asymmetrical stretch of the carboxylate group may be responsible for the stronger band at 1635  $\text{cm}^{-1}$ . The band that is present at 1311  $\text{cm}^{-1}$  is what causes the carboxylate group to extend in a symmetrical manner. According to Jung *et al.*, (2000) and Ding *et al.*, (2000), the ether C-O stretching vibration resulted in formation of peak at 1068 $\text{cm}^{-1}$  and that of alcoholic group at 1028  $\text{cm}^{-1}$ , and 500 to 900  $\text{cm}^{-1}$  Ti-O-Ti. Catechin/silver/ $\text{TiO}_2$  nanoparticles' spectra, however, displayed distinctive absorbance bands at 3416, 2920, 2852, 2326, 2111, 1635, 1462, 1384, 1097, 1018, 663, and 606. The hydroxyl group's stretching vibration and the water molecules interlayer can be linked to the shift in absorbance peaks that was seen in the IR spectrum of nanoparticles (Liu *et al.*, 2007). The major key contributors to this phenomenon were (a) Ti-O-H stretching vibration and (b) powder surface adsorption.

According to Li *et al.*, (2008), for all samples, the band near 1635  $\text{cm}^{-1}$  can be attributed to the bending vibration of the H-O-H bond on the titanium dioxide catalyst, and the band at 1384  $\text{cm}^{-1}$

indicates the binding of Ag-O-Ti, respectively. Furthermore, the existence of transitional metal carbonyls at the peaks at 2326 cm and 2111 cm confirms that the oxidation of the hydroxyl and carbonyl groups is connected to reduction of the silver ions, indicating that the catechin is more thoroughly oxidized. It may be comprehended that the carbonyl and hydroxyl groups of catechin are actively involved in the creation of Ag NPs depending up on the band shift in these groups, there may be a loss of any existing carbonyl, or may be an emergence of a new carbonyl peak. The band at  $1462\text{cm}^{-1}$  corresponds to asymmetric (Djaoued *et al.*, 2002) and that at  $663\text{cm}^{-1}$  denotes anatase peak of  $\text{TiO}_2$ .

The energy dispersive spectroscopy (EDS) analysis of the  $\text{TiO}_2$  nanoparticles confirmed the presence of elemental metal signal (Figure 4). The shape of the titanium dioxide nanoparticles was seen in the scanning electron micrograph and was roughly spherical, indicating that they were aggregated. When viewed closely, it was clearly evident that the powder particles seemed to be slightly aggregated (Figure 5a & 5b).

Poly disperse nanoparticles with spherical forms could be seen in the TEM images (Figure 6a). The TEM micrograph of the  $\text{TiO}_2$  NPs generated using silver and acacia extract clearly shows that each individual nanoparticle has a nearly spherical shape and measures 232 nm in size. Our experimental results confirm the effective manufacture of smaller anatase  $\text{TiO}_2$  nanoparticles as compared to the literature report (Prasad *et al.*, 2007). Titanium ions have been transformed into metallic nanoparticles by catechin. According to Sasaki *et al.*, (2004), a distinct diffraction rings that corresponded to the anatase phase were displayed by the selected area electron diffraction SAED pattern (Figure 6b).

$\text{TiO}_2$  particles can be utilized in paints and coatings, sunscreens, energy storage devices, and other products (Wang *et al.*, 2007; Vargas *et al.*, 2006; Wildeson *et al.*, 2008). Rutile, brookite, and anatase are the three crystalline phases of  $\text{TiO}_2$  that can be produced. The latter are the materials for photocatalysis that have been investigated the most, and each one has unique features and consequently distinct applications (Boccaccini *et al.*, 2004).  $\text{TiO}_2$  NPs are regarded as a superior band-gap semiconductor, much like ZnO NPs (Ju-Nam and Lead, 2008).  $\text{TiO}_2$  nanoparticles, on the other hand, frequently agglomerate. Due to their potential oxidation strength, high photo stability, and lack of toxicity,  $\text{TiO}_2$  nanoparticles outstand among the various other metal oxide nanoparticles in terms of their intense range of applications in air as well as water purification, DSSC, and other fields (Li *et al.*, 2004, Al-Salim *et al.*, 2010, and Ito *et al.*, 1999). Therefore, in this study, we prepared unique nano compounds that can be employed as antifouling chemicals using  $\text{TiO}_2$  and Ag.

The silver nanoparticles are effective (Kwok and Leung, 2005) and mercuric chloride (Wisley and Blick, 1967) and is ecofriendly chemical and less hazardous to the marine environment. The catechin from *Acacia catechu* showed highest inhibitory activity against the biofilms in our earlier studies, so catechin and silver along with Titania is used to prepare a hybrid compound CAT nanoparticle. Surprisingly it showed the best results compared to toxic chemicals which were used as controls in this experiment, The CAT nanoparticles are 10 times more effective when compared to the control copper sulphate and mercuric chloride (Figure 7) and is ecofriendly chemical and less hazardous to the marine environment.

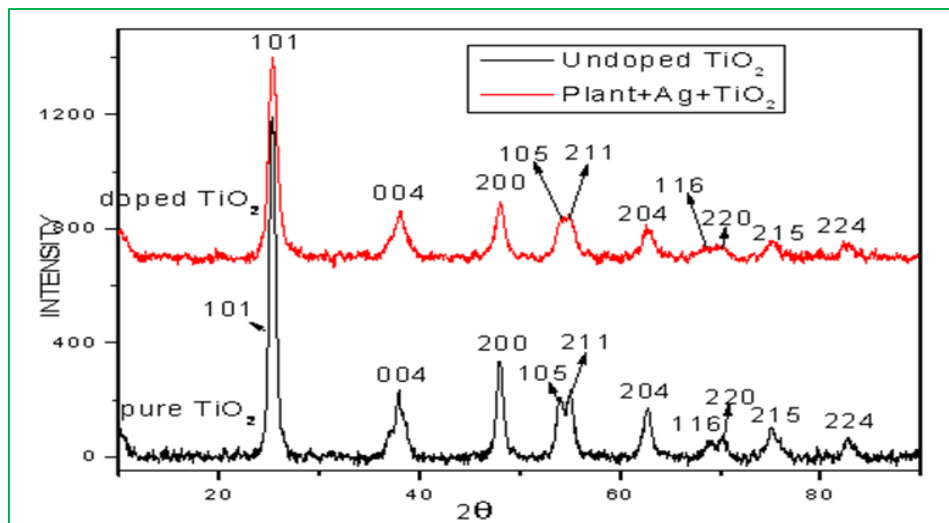


Figure 1: Powder X-ray Diffraction XRD patterns of C/Ag/TiO<sub>2</sub> Nanoparticles.

Table 1: Lattice parameters

	2θ	d	FWHM of intense peak β (radians)	Size of the crystallite (D) nm	Lattice Parameters	hkl
Pure TiO <sub>2</sub>	25.28	3.520	0.0083	17	a=b=3.7852 c=9.5139	101
Catechin/Ag Doped TiO <sub>2</sub>	25.35	3.511	0.0166	9	a=b=3.780 c=9.444	101

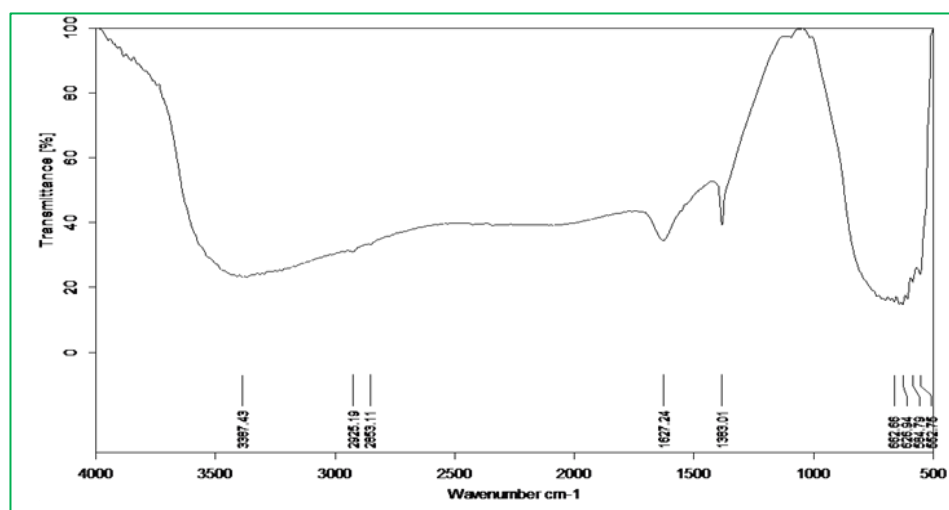


Figure 2: FT-IR of pure TiO<sub>2</sub>

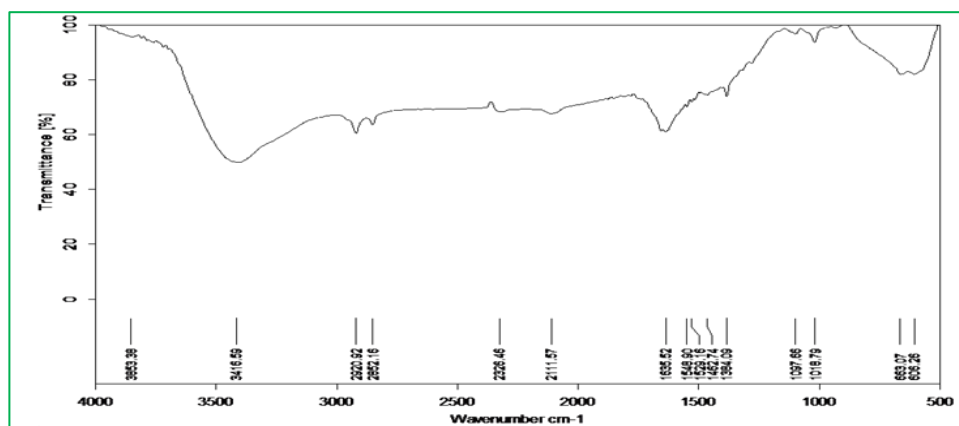


Figure 3: FT-IR of Catechi-Ag-TiO<sub>2</sub>

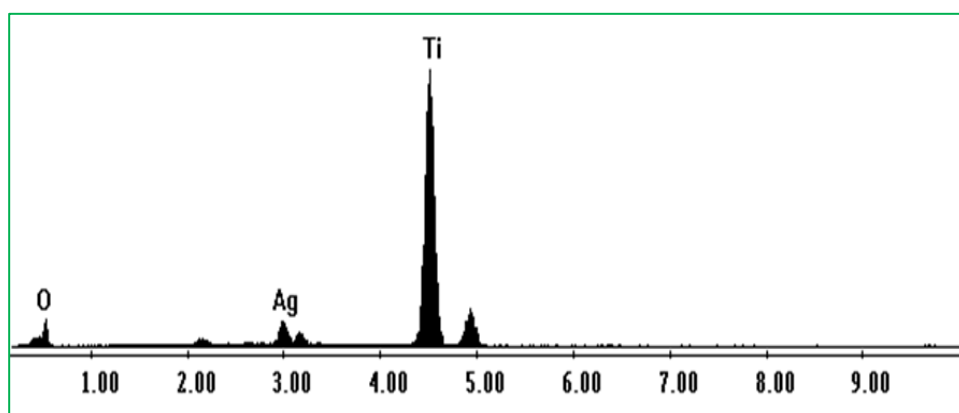


Figure 4: Energy Dispersive Spectrometry (EDS)

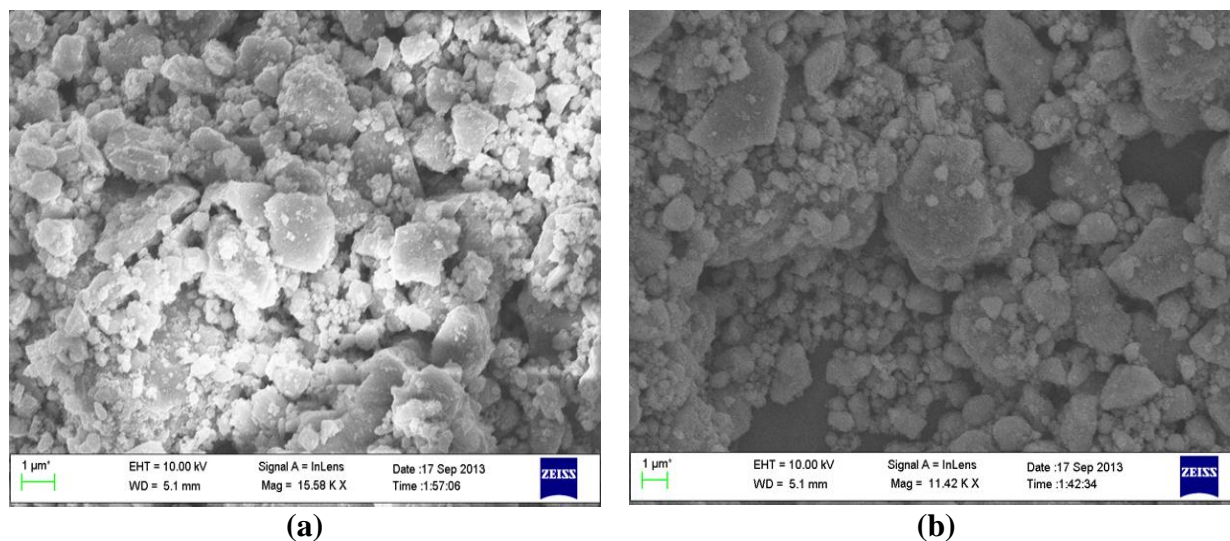
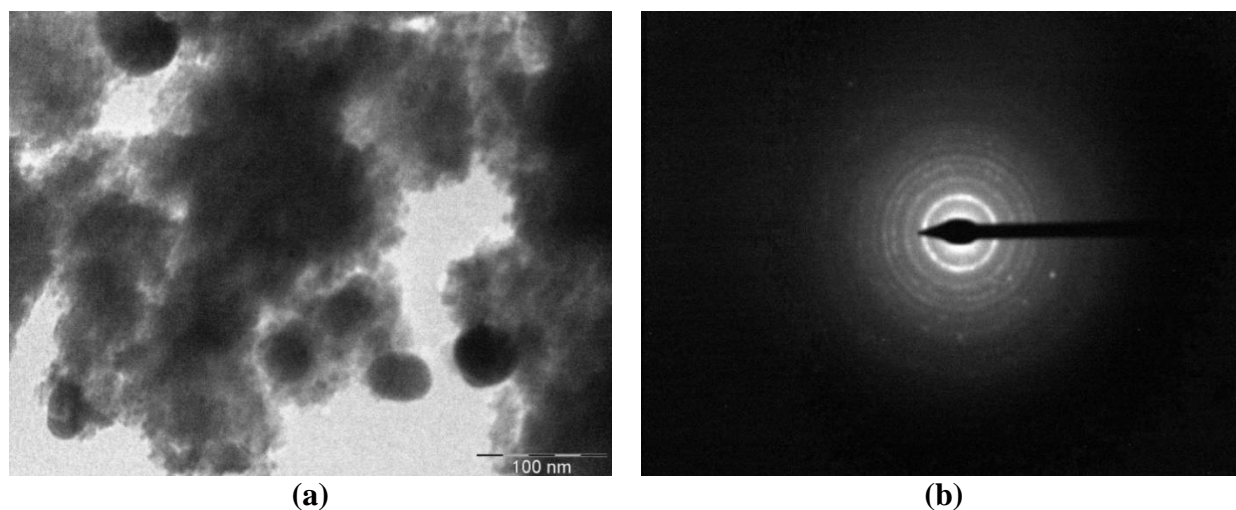
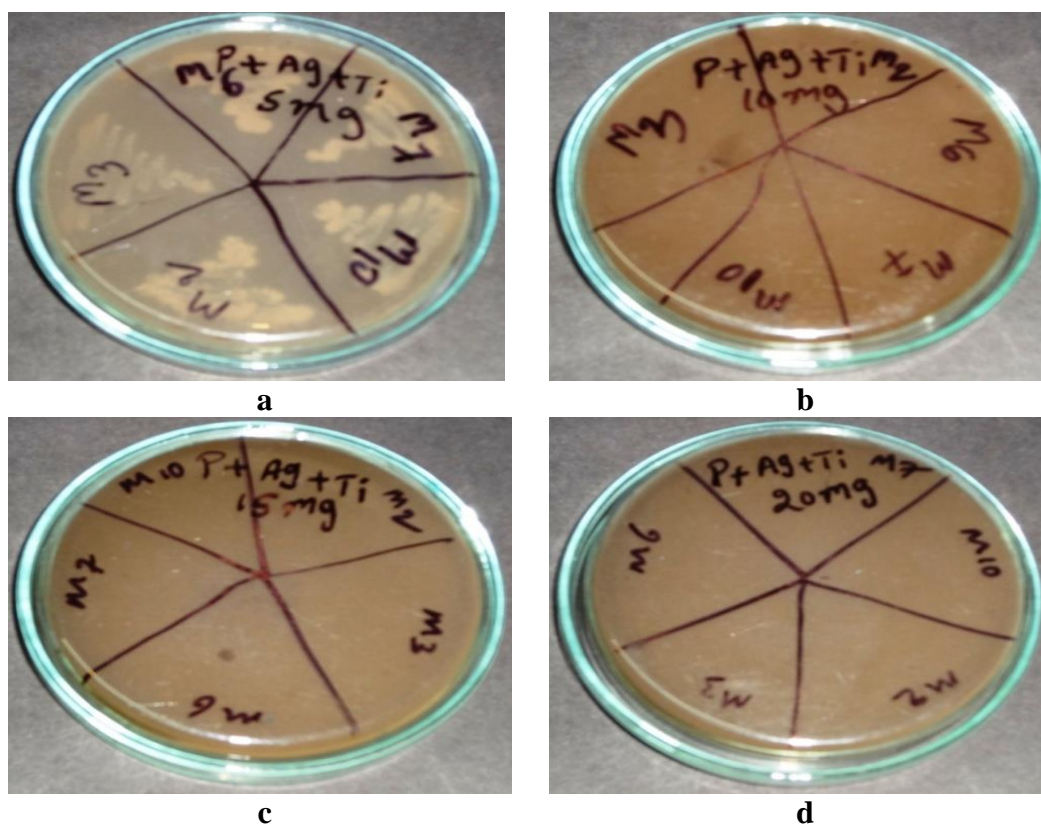


Figure 5: (a) FE-SEM micrograph of Catechin/ Silver/ TiO<sub>2</sub> nanoparticles (b) FE-SEM micrograph of pure TiO<sub>2</sub>.



**Figure 6:** (a) TEM micrograph of Catechin/Ag/TiO<sub>2</sub> and (b) the selected area electron diffraction pattern of Catechin/ Ag/TiO<sub>2</sub> Nanoparticles.



**Figure 7:** Determination of Minimum Inhibitory Concentrations (MICs) by agar dilution method: the concentration decreasing from 20 mg 10 ml<sup>-1</sup> to 5 mg 10 ml<sup>-1</sup> is tested, growth is observed up to 5 mg 10 ml<sup>-1</sup> and the growth is inhibited at 10 mg 10 ml<sup>-1</sup>, the final MIC is 1.0 mg ml<sup>-1</sup>.



### Conclusion

All maritime industrial equipment has a significant operational problem when it comes to controlling marine microfouling and its detrimental impact on submerged surfaces. From this finding, it may be inferred that Catechin-silver-Titania nanoparticles may contribute to biofilm prevention. This work also demonstrates the synergistic effect of CAT nanoparticles against biofilm forming bacteria. In comparison to the test compounds, the synthesized new CAT NPs demonstrated the best results. CAT NPs may be coated on marine industrial surfaces in order to take use of its potential antifouling activity.

### Acknowledgement

Authors greatly acknowledge the UGC, for the financial support under RGNF scheme, and thankful to the institution for providing the laboratory facilities.

### References

1. Adams, L.K., Lyon, D.Y. and Alvarez, P.J. (2006). Comparative eco-toxicity of nanoscale TiO<sub>2</sub>, SiO<sub>2</sub>, and ZnO water suspensions. *Water Research*, 40(19), 3527-3532.
2. Ahmad, N., Sharma, S., Alam, M.K., Singh, V.N., Shamsi, S.F., Mehta, B.R. and Fatma, A. (2010). Rapid synthesis of silver nanoparticles using dried medicinal plant of basil. *Colloids and Surfaces B: Biointerfaces*, 81(1), 81-86.
3. Akhavan, O. (2009). Lasting antibacterial activities of Ag-TiO<sub>2</sub>/Ag/a-TiO<sub>2</sub> nanocomposite thin film photocatalysts under solar light irradiation. *Journal of Colloid and Interface Science*, 336(1), 117-124.
4. Al-Salim, N.I., Bagshaw, S.A., Bittar, A., Kemmitt, T., McQuillan, A.J., Mills, A.M. and Ryan, M.J. (2000). Characterisation and activity of sol-gel-prepared TiO<sub>2</sub> photocatalysts modified with Ca, Sr or Ba ion additives. *Journal of Materials Chemistry*, 10(10), 2358-2363.
5. Badawy, A.M.E., Luxton, T.P., Silva, R.G., Scheckel, K.G., Suidan, M.T. and Tolaymat, T.M. (2010). Impact of environmental conditions (pH, ionic strength, and electrolyte type) on the surface charge and aggregation of silver nanoparticles suspensions. *Environmental Science and Technology*, 44(4), 1260-1266.
6. Boccaccini, A.R., Karapappas, P., Marijuan, J.M. and Kaya, C. (2004). TiO<sub>2</sub> coatings on silicon carbide and carbon fibre substrates by electrophoretic deposition. *Journal of Materials Science*, 39, 851-859.
7. Breggin, L.K. and Pendergrass, J. (2007). Where does the nano go?: end-of-life regulation of nanotechnologies. Washington, DC: Project on Emerging Nanotechnologies at the Woodrow Wilson International Center for Scholars.
8. Castro, L., Reyes, P. and de Correa, C.M. (2002). Synthesis and Characterization of Sol-Gel Cu-ZrO<sub>2</sub> and Fe-ZrO<sub>2</sub> Catalysts. *Journal of Sol-Gel Science and Technology*, 25, 159-168.
9. Chao, H.E., Yun, Y.U., Xingfang, H.U. and Larbot, A. (2003). Effect of silver doping on the phase transformation and grain growth of sol-gel titania powder. *Journal of the European Ceramic Society*, 23(9), 1457-1464.

10. Chaudhari, P.R., Masurkar, S.A., Shidore, V.B. and Kamble, S.P. (2012). Effect of biosynthesized silver nanoparticles on *Staphylococcus aureus* biofilm quenching and prevention of biofilm formation. *Nano-Micro Letters*, 4, 34-39.
11. Cozzoli, P.D., Comparelli, R., Fanizza, E., Curri, M.L., Agostiano, A. and Laub, D. (2004). Photocatalytic synthesis of silver nanoparticles stabilized by TiO<sub>2</sub> nanorods: A semiconductor/metal nanocomposite in homogeneous nonpolar solution. *Journal of the American Chemical Society*, 126(12), 3868-3879.
12. Dhage, S.R., Gaikwad, S.P. and Ravi, V. (2004). Synthesis of nanocrystalline TiO<sub>2</sub> by tartarate gel method. *Bulletin of Materials Science*, 27, 487-489.
13. Ding, Z., Lu, G.Q. and Greenfield, P.F. (2000). Role of the crystallite phase of TiO<sub>2</sub> in heterogeneous photocatalysis for phenol oxidation in water. *The Journal of Physical Chemistry B*, 104(19), 4815-4820.
14. Djaoued, Y., Badilescu, S., Ashrit, P.V., Bersani, D., Lottici, P.P. and Brüning, R. (2002). Low temperature sol-gel preparation of nanocrystalline TiO<sub>2</sub> thin films. *Journal of Sol-Gel Science and Technology*, 24, 247-254.
15. Ge, L., Xu, M., Sun, M. and Fang, H. (2006). Low-temperature synthesis of photocatalytic TiO<sub>2</sub> thin film from aqueous anatase precursor sols. *Journal of Sol-Gel Science and Technology*, 38, 47-53.
16. Guin, D., Manorama, S.V., Latha, J.N.L. and Singh, S. (2007). Photoreduction of silver on bare and colloidal TiO<sub>2</sub> nanoparticles/nanotubes: synthesis, characterization, and tested for antibacterial outcome. *The Journal of Physical Chemistry C*, 111(36), 13393-13397.
17. Ito, S., Inoue, S., Kawada, H., Hara, M., Iwasaki, M. and Tada, H. (1999). Low-temperature synthesis of nanometer-sized crystalline TiO<sub>2</sub> particles and their photo induced decomposition of formic acid. *Journal of Colloid and Interface Science*, 216(1), 59-64.
18. Jha, A.K., Prasad, K. and Kulkarni, A.R. (2009). Synthesis of TiO<sub>2</sub> nanoparticles using microorganisms. *Colloids and Surfaces B: Biointerfaces*, 71(2), 226-229.
19. Ju-Nam, Y. and Lead, J.R. (2008). Manufactured nanoparticles: an overview of their chemistry, interactions and potential environmental implications. *Science of the Total Environment*, 400(1-3), 396-414.
20. Jung, K.Y. and Park, S.B. (2000). Enhanced photoactivity of silica-embedded titania particles prepared by sol-gel process for the decomposition of trichloroethylene. *Applied Catalysis B: Environmental*, 25(4), 249-256.
21. Kalimuthu, K., Babu, R.S., Venkataraman, D., Bilal, M. and Gurunathan, S. (2008). Biosynthesis of silver nanocrystals by *Bacillus licheniformis*. *Colloids and surfaces B: Biointerfaces*, 65(1), 150-153.
22. Kathiresan, K., Manivannan, S., Nabeel, M.A. and Dhivya, B. (2009). Studies on silver nanoparticles synthesized by a marine fungus, *Penicillium fellutanum* isolated from coastal mangrove sediment. *Colloids and surfaces B: Biointerfaces*, 71(1), 133-137.

23. Kirthi, A.V., Rahuman, A.A., Rajakumar, G., Marimuthu, S., Santhoshkumar, T., Jayaseelan, C. and Bagavan, A. (2011). Biosynthesis of titanium dioxide nanoparticles using bacterium *Bacillus subtilis*. *Materials Letters*, 65(17-18), 2745-2747.
24. Krishna, V., Noguchi, N., Koopman, B. and Moudgil, B. (2006). Enhancement of titanium dioxide photocatalysis by water-soluble fullerenes. *Journal of Colloid and Interface Science*, 304(1), 166-171.
25. Kwok, K.W.H. and Leung, K.M. (2005). Toxicity of antifouling biocides to the intertidal harpacticoid copepod *Tigriopus japonicus* (Crustacea, Copepoda): effects of temperature and salinity. *Marine Pollution Bulletin*, 51(8-12), 830-837.
26. Li, Y., Ma, G., Peng, S., Lu, G. and Li, S. (2008). Boron and nitrogen co-doped titania with enhanced visible-light photocatalytic activity for hydrogen evolution. *Applied Surface Science*, 254(21), 6831-6836.
27. Li, Y., White, T.J. and Lim, S.H. (2004). Low-temperature synthesis and microstructural control of titanium nano-particles. *Journal of Solid State Chemistry*, 177(4-5), 1372-1381.
28. Liu, J., Li, X., Zuo, S. and Yu, Y. (2007). Preparation and photocatalytic activity of silver and TiO<sub>2</sub> nanoparticles/montmorillonite composites. *Applied Clay Science*, 37(3-4), 275-280.
29. Long, M., Cai, W., Wang, Z. and Liu, G. (2006). Correlation of electronic structures and crystal structures with photocatalytic properties of undoped, N-doped and I-doped TiO<sub>2</sub>. *Chemical Physics Letters*, 420(1-3), 71-76.
30. Masuda, Y. and Kato, K. (2009). Synthesis and phase transformation of TiO<sub>2</sub> nano-crystals in aqueous solutions. *Journal of the Ceramic Society of Japan*, 117(1363), 373-376.
31. Masurkar, S.A., Chaudhari, P.R., Shidore, V.B. and Kamble, S.P. (2011). Rapid biosynthesis of silver nanoparticles using *Cymbopogon citratus* (lemongrass) and its antimicrobial activity. *Nano-Micro Letters*, 3, 189-194.
32. Mills, A., Davies, R.H. and Worsley, D. (1993). Water purification by semiconductor photocatalysis. *Chemical Society Reviews*, 22(6), 417-425.
33. Novitsky, J.A. and MacSween, M.C. (1989). Microbiology of a high energy beach sediment: Evidence for an active and growing community. *Marine Ecology Progress Series*. Oldendorf, 52(1), 71-75.
34. Prasad, K., Jha, A.K. and Kulkarni, A.R. (2007). Lactobacillus assisted synthesis of titanium nanoparticles. *Nanoscale Research Letters*, 2, 248-250.
35. Raut, R.W., Kolekar, N.S., Lakkakula, J.R., Mendhulkar, V.D. and Kashid, S.B. (2010). Extracellular synthesis of silver nanoparticles using dried leaves of *Pongamiapinnata* (L) pierre. *Nano-Micro Letters*, 2, 106-113.
36. Rolison, D.R. (2003). Catalytic nanoarchitectures-the importance of nothing and the unimportance of periodicity. *Science*, 299(5613), 1698-1701.

37. Saifuddin, N., Wong, C.W. and Yasumira, A.A. (2009). Rapid biosynthesis of silver nanoparticles using culture supernatant of bacteria with microwave irradiation. *E-journal of Chemistry*, 6(1), 61-70.
38. Sasaki, T., Liang, C., Nichols, W.T., Shimizu, Y. and Koshizaki, N. (2004). Fabrication of oxide base nanostructures using pulsed laser ablation in aqueous solutions. *Applied Physics A*, 79, 1489-1492.
39. Schmid, G. (2011). Metal nanoparticles, synthesis of. *Encyclopedia of Inorganic Chemistry*.
40. Sundrarajan, M. and Gowri, S. (2011). Green synthesis of titanium dioxide nanoparticles by *Nyctanthes arbor-tristis* leaves extract. *Chalcogenide Letters*, 8(8), 447-451.
41. Tiede, K., Hassellöv, M., Breitbarth, E., Chaudhry, Q. and Boxall, A.B. (2009). Considerations for environmental fate and ecotoxicity testing to support environmental risk assessments for engineered nanoparticles. *Journal of chromatography A*, 1216(3), 503-509.
42. Vargas, W.E., Amador, A. and Niklasson, G.A. (2006). Diffuse reflectance of TiO<sub>2</sub> pigmented paints: Spectral dependence of the average path length parameter and the forward scattering ratio. *Optics Communications*, 261(1), 71-78.
43. Velayutham, K., Rahuman, A.A., Rajakumar, G., Santhoshkumar, T., Marimuthu, S., Jayaseelan, C. and Elango, G. (2012). Evaluation of *Catharanthus roseus* leaf extract-mediated biosynthesis of titanium dioxide nanoparticles against *Hippobosca maculata* and *Bovicolaovis*. *Parasitology Research*, 111, 2329-2337.
44. Vidhu, V.K., Aromal, S.A. and Philip, D. (2011). Green synthesis of silver nanoparticles using *Macrotylomauniflorum*. *Spectrochimica Acta Part A: Molecular and Biomolecular Spectroscopy*, 83(1), 392-397.
45. Wang, G. (2007). Hydrothermal synthesis and photo catalytic activity of nanocrystalline TiO<sub>2</sub> powders in ethanol–water mixed solutions. *Journal of Molecular Catalysis A: Chemical*, 274(1-2), 185-191.
46. Wildeson, J., Smith, A., Gong, X., Davis, H.T. and Scriven, L.E. (2008). Understanding and improvement of TiO<sub>2</sub> efficiency in waterborne paints through latex design. *Jct Coatings Tech*, 5(7), 32.
47. Wisely, B. and Blick, R.A.P. (1967). Mortality of marine invertebrate larvae in mercury, copper, and zinc solutions. *Marine and Freshwater Research*, 18(1), 63-72.